Interfacially Initiated Microemulsion Copolymerization: One-Stage Preparation of Poly(*n*-butyl methacrylate)–Poly(*N*-vinyl pyrrolidone) Core–Shell Nanoparticles

Wei-Dong He, Cheng Zheng, Fang-Mao Ye, Yan-Mei Wang, Wei-Jun Liu

Department of Polymer Science and Engineering, University of Science and Technology of China, Hefei, Anhui 230026, China

Received 21 September 2005; accepted 15 October 2005
DOI 10.1002/app.23445
Publication online in Wiley InterScience (www.interscience.wiley.com).

ABSTRACT: Interfacially initiated microemulsion copolymerizations of *n*-butyl methacrylate (BMA) and *N*-vinyl pyrrolidone (NVP) by the redox initiation couple of benzoyl peroxide and ferrous sulfate were carried out with Tween 80 and *n*-butanol as the surfactant and cosurfactant, respectively. Fourier transform infrared spectroscopy and X-ray photoelectron spectroscopy were recorded to analyze the chemical composition of the latex particles. Transmission electron microscopy was used to observe the particle morphology and dynamic light scattering to determine the particle size. The results demonstrated that interfacially initiated microemulsion polymerization prompted the copolymerization of the water-soluble NVP monomer with the oil-soluble BMA monomer to form core–shell nanoparticles. The influence of the surfactant concentration, BMA amount, and temperature on the particle size and polymerization rate was investigated. © 2006 Wiley Periodicals, Inc. J Appl Polym Sci 101: 3751–3757, 2006

Key words: core–shell polymers; interfaces; nanoparticles

INTRODUCTION

A microemulsion is a transparent/translucent and thermodynamically stable system, and many applications have been found in a variety of areas, such as oil recovery, microreactors, and controlled drug release.[1–4] A lot of effort has been devoted to revealing the characteristics of microemulsion polymerizations, including the kinetics, nucleation, and initiation loci.[5–8]

Both oil-soluble and water-soluble initiators are used in oil-in-water microemulsion polymerization. Generally, the initiation locus of microemulsion polymerization is considered the microemulsion droplet. The initiation involves two events: the formation of initiating radicals by the decomposition of the initiator in the reaction medium and the entry of oligomeric radicals into the micelles. As for oil-soluble initiators, the initiating radicals result from the desorption of primary radicals in the micelles or the decomposition of initiators in water.[9] Redox initiators have also been used. The microemulsion polymerization of styrene has been kinetically studied with potassium persulfate (KPS)/*p*-methyl benzaldehyde sodium bisulfite adduct as the redox initiation couple.[10] Xu et al.[11] prepared a nanosized polymeric latex with a high polymer/emulsifier ratio with ammonium persulfate and tetramethylethylenediamine as the initiators of microemulsion polymerization. Microemulsion copolymerizations have also been studied by several research groups, but few reports have been published concerning the copolymerizations of a water-soluble monomer and an oil-soluble monomer. Puig et al.[12] reported the copolymerization of styrene and acrylic acid in a cationic microemulsion, and an overall conversion of only 60% was reached. Pokhriyal and coworkers[13,14] studied the kinetics and behavior of the microemulsion copolymerization of a hydrophobic monomer of 2-ethylhexyl acrylate and a partially hydrophilic monomer of acrylonitrile.

Emulsion polymerization initiated with a redox mixture composed of an oil-soluble component and a water-soluble component is a good way of producing hydrophobic-core/hydrophilic-shell composite latices.[15–17] In our previous article,[18] in which microemulsion polymerization initiated in this way was called interfacially initiated microemulsion polymerization, we carried out the copolymerization of the oil-soluble monomer *n*-butyl methacrylate (BMA) and the water-soluble monomer *N*-vinyl pyrrolidone (NVP). In this article, we confirm that interfacially initiated microemulsion polymerization prompts the copolymerization of BMA and NVP and the formation of core–shell nanoparticles. The influence of the surfactant concen-

Correspondence to: W.-D. He (wdhe@ustc.edu.cn).
Contract grant sponsor: Natural Science Foundation of Anhui Province; contract grant number: 01044906.

tration, BMA amount, and temperature on the particle size and polymerization rate (R_p) is investigated.

EXPERIMENTAL

Materials

NVP (Tokyo Kasei Kogyo, Tokyo, Japan) was distilled *in vacuo* before use. BMA was washed with an aqueous NaOH (10 wt %) solution and then with distilled water until pH 7. After being dried with anhydrous $MgSO_4$, BMA was distilled *in vacuo* before use. Benzoyl peroxide (BPO) and KPS were analytical reagents and were purified by recrystallization. Polyoxyethylene ($n = 20$) sorbitan monooleate (Tween 80), *n*-butanol, and ferrous sulfate hydrate ($FeSO_4 \cdot 7H_2O$) were analytical reagents and were used as received.

Interfacially initiated microemulsion polymerization

Interfacially initiated microemulsion copolymerizations of BMA and NVP were carried out with a modified procedure similar to that reported in ref. 18. Briefly, BPO (30.0 mg) was dissolved in BMA, and the resultant solution was emulsified in an aqueous solution of Tween 80 and butanol (0.40 g) to form a clear or translucent microemulsion. The amount of water in the Tween 80 solution was varied to make the total weight of the reaction mixture 50.0 g. After being heated to a certain temperature while being purged with nitrogen, the microemulsion was charged with an aqueous solution (5.0 mL) of NVP and $FeSO_4 \cdot 7H_2O$ (40 mg) in a batch. The reaction lasted for another 12 h and resulted in a composite latex of poly(*n*-butyl methacrylate) (PBMA) and poly(*N*-vinyl pyrrolidone) (PNVP). PBMA–PNVP solid particles were obtained by de-emulsification with ethanol, washed with ethanol, and dried *in vacuo*. Noninterfacially initiated microemulsion copolymerizations with KPS–$FeSO_4$ were also performed in the same way for comparison. The continuous addition of an NVP/$FeSO_4$ solution was performed with an Sp1001 syringe pump (Sarasota, FL).

Determination of the monomer conversion and kinetic study

After the polymerization, water, butanol, and unreacted monomer were removed *in vacuo* at 35°C until the weight of the remaining substances was constant. The solid content of latex (SC) was obtained, and the overall monomer conversion (Con) was calculated as follows:

$$\text{Con} = \frac{\text{SC} \times G - A - B}{W_1 + W_2} \times 100\% \qquad (1)$$

where G, A, B, W_1, and W_2 are the amounts of the total latex, emulsifiers, initiator(s), BMA, and NVP, respectively.

To follow the polymerization conversion, a portion of the latex was taken out at different intervals and added to a 1,4-diphenol solution. The mixture then was dried *in vacuo* until no weight change was observed. Con was calculated in the same way as before, with consideration given to the addition of 1,4-diphenol.

Chemical composition of the PBMA–PNVP latex particles

To confirm the copolymerization of BMA and NVP, PBMA–PNVP solid particles were extracted with water for 5 days and dried *in vacuo*. Their Fourier transform infrared (FTIR) spectra were recorded on a Bruker Vector-22 infrared spectrometer (Ettlingen, Germany) with KBr pellets. Also, X-ray photoelectron spectroscopy (XPS) measurements of extracted PBMA–PNVP solid particles were performed on a VG Escalab MKII X-ray photoelectron spectrometer (UK) with nonmonochromatic Al Kα radiation (1486.6 eV) under high vacuum of 10^{-11} mbar.

Morphology and size of the PBMA–PNVP latex particles

A few drops of the diluted PBMA–PNVP latex were dropped onto a copper grid. After the evaporation of water, the morphology of the PBMA–PNVP latex particles was observed with transmission electron microscopy (TEM; model H-800, Hitachi, Tokyo, Japan) at an accelerating voltage of 200 kV.

Dynamic laser light scattering (LLS) was performed on a modified commercial LLS spectrometer (ALV/SP-125, Germany) equipped with an ALV-5000 multi-τ digital time correlator and a He–Ne laser (output power = 10 mW at 632 nm) at 25°C to get the size of the PBMA–PNVP latex particles. Before dynamic light scattering (DLS) measurement, the latex was diluted with distilled water to a given concentration, and a filter (0.45 μm) was used to eliminate any dust. The Laplace inversion of the intensity–intensity time correlation function [$G^{(2)}(t,q)$] in the self-beating mode resulted in a line width distribution [$G(\Gamma)$]. $G(\Gamma)$ was directly converted to the hydrodynamic radius distribution [$f(R_h)$] with the Stokes–Einstein equation: $R_h = k_BT/(6\pi\eta D)$, where R_h, k_B, T, η, and D are the hydrodynamic radius, Boltzman constant, absolute temperature, solvent viscosity, and translational diffusion coefficient, respectively. The polydispersity index (PDI) of R_h was defined as follows:[19]

$$\text{PDI} = \mu_2/\bar{\Gamma}^2 \qquad (2)$$

TABLE I
Effects of the Temperature on the Microemulsion Polymerization

Latex	Initiators (mg)			Temperature (°C)	Addition of the water-soluble components	Particle size	
	BPO	KPS	$FeSO_4 \cdot 7H_2O$			R_h (nm)	PDI
Y-213	—	30	—	65	Batch	32	0.048
Y-210	30	—	—	65	Batch	41	0.054
Y-301	30	—	40	40	Batch	20	0.064
Y-221	—	30	40	40	Batch	18	0.106
Y-307	30	—	40	40	Continuous	24	0.034

The polymerizations of BMA (5.0 g) and NVP (0.5 g) were carried out with BPO or KPS (30 mg), $FeSO_4 \cdot 7H_2O$ (40 g), Tween 80 (3.00 g), and *n*-butanol (0.40 g) at different temperature for 12 h. The total weight of the reaction mixture was 50.0 g. The $FeSO_4$/NVP solution was added in a batch.

where

$$\mu_2 = \int (\tau - \bar{\tau})^2 G(G) d\tau \quad (3)$$

RESULTS AND DISCUSSION

Chemical composition of the PBMA–PNVP latex particles

Interfacially initiated microemulsion polymerization is suggested in our previous article.[18] BPO and BMA are oil-soluble and stay in the micelles and latex particles, whereas NVP and $FeSO_4$ are water-soluble and exist in the aqueous medium. Additionally, NVP coordinates with Fe^{2+} in the aqueous medium; this has been confirmed by the formation of a red solution when an aqueous $FeSO_4$ solution is added to NVP. The redox reaction between BPO and $FeSO_4$ occurs at the interface at which their encounter takes place. Therefore, the primary radicals are formed mainly at the interface. This radical formation method helps the copolymerization of BMA and NVP near the interface. Otherwise, primary radicals are formed in the oil phase or in the water phase for other microemulsion polymerizations.

Different microemulsion copolymerizations have been carried out, as shown in Table I. Microemulsion polymerizations initiated by redox initiation couples have much higher R_p values and lower particle sizes than those initiated by single-component initiators. Compared with the polymerization initiated with KPS/Fe^{2+}, interfacially initiated microemulsion polymerization has a higher R_p value and larger particle size.[18]

FTIR spectra of different extracted PBMA–PNVP latex particles are shown in Figure 1. Their FTIR spectra display the characteristic absorption band attributed to the carbonyl stretching vibration of BMA at 1730 cm^{-1} and those attributed to C—O of aliphatic ester at 1260 and 1160 cm^{-1}. The absorption bands attributed to the carbonyl stretching vibration and

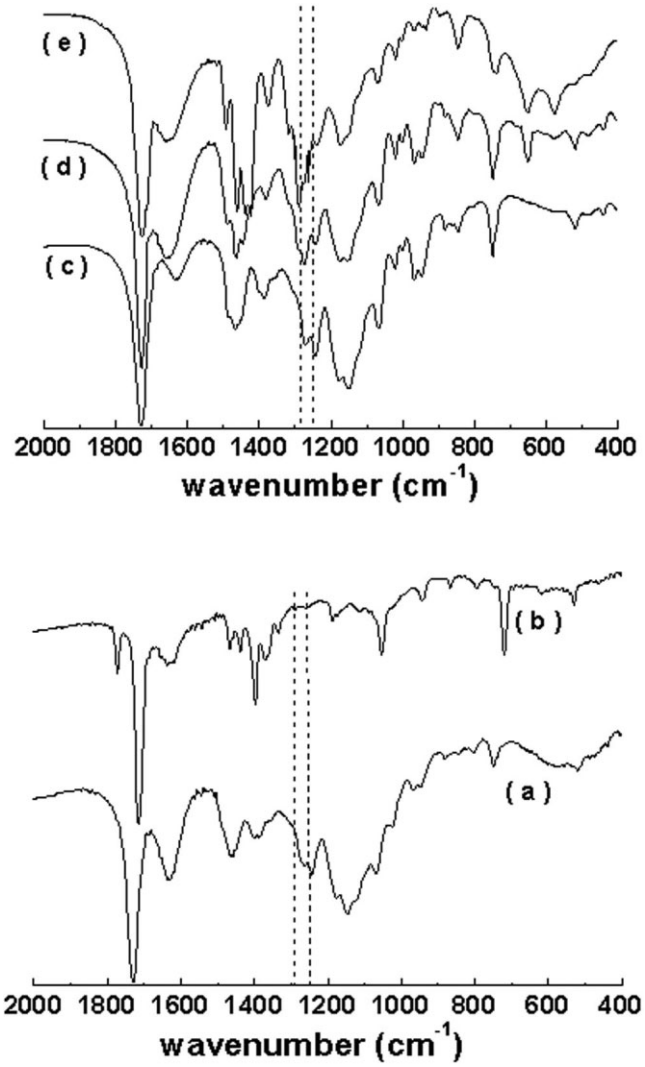

Figure 1 FTIR spectra of different latex particles after extraction with water: (a) initiated by KPS at 65°C, (b) initiated by BPO at 65°C, (c) initiated by KPS–$FeSO_4$ at 40°C, and (d) initiated by BPO–$FeSO_4$ at 40°C with the batch addition of $FeSO_4$–NVP and (e) initiated by BPO–$FeSO_4$ at 40°C with the continuous addition of $FeSO_4$–NVP.

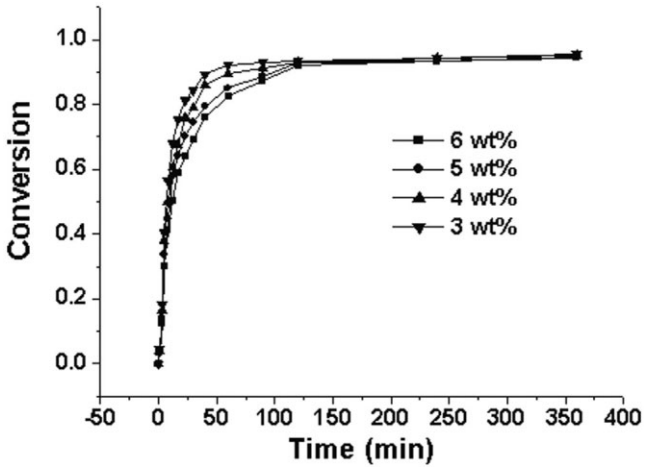

Figure 2 Conversion versus the time at different surfactant concentrations with the batch addition of an $FeSO_4$/NVP solution: (■) 6, (●) 5, (▲) 4, and (▼) 3 wt %.

C—N stretching vibration of NVP appear at 1670 and 1290 cm^{-1}, respectively. The intensity of the absorption band at 1290 cm^{-1} is weaker than that at 1260 cm^{-1}, indicating that NVP hardly copolymerizes with BMA when a single-component initiator is used, especially BPO. On the contrary, the relative intensity of the absorption band at 1290 cm^{-1} increases obviously when redox initiators are used. As for the interfacially initiated microemulsion copolymerization with BPO/$FeSO_4$, the intensity of the absorption band at 1290 cm^{-1} exceeds that at 1260 cm^{-1}. This result confirms that interfacially initiated microemulsion polymerization facilitates the copolymerization of NVP and BMA. In addition, the continuous addition of the water-soluble components NVP and $FeSO_4$ to the polymerization mixture further prompts the copolymerization according to a comparison of Figure 2(d,e). In our previous study,[18] we discussed the influence of the addition of $FeSO_4$–NVP and found that bigger latex particles resulted from the higher tendency for the copolymerization of NVP and BMA.

Influence of the surfactant concentration on the interfacially initiated microemulsion polymerization of BMA/NVP

In a typical microemulsion polymerization, the surfactant concentration is 10% or more with respect to the total weight of the latex and has a significant influence on the R_p value, latex particle size, and molecular weight of the resultant polymer. Many attempts have been devoted to reducing the surfactant concentration in microemulsion polymerization.

We prepared BMA microemulsions with different Tween concentrations (2.0–6.0 wt %), and all the mixtures were transparent even though an $FeSO_4$/NVP solution was added. Further reducing the surfactant concentration led to a milky or white emulsion. Thus, microemulsion copolymerizations of BMA and NVP with different surfactant concentrations with the batch addition of an $FeSO_4$/NVP solution were also carried out, and the results are summarized in Table II. With the reduction of the Tween 80 concentration from 6.0 to 2.0 wt %, the particle sizes for both interfacially initiated microemulsion polymerizations with BPO–Fe^{2+} and noninterfacially initiated microemulsion polymerizations with KPS–Fe^{2+} increased, and the particle size distribution became broader. With the same Tween 80 concentration, interfacially initiated microemulsion polymerization resulted in larger latex particles with narrower size distributions.

Figure 2 demonstrates the monomer conversion change versus the time in the interfacially initiated microemulsion copolymerizations of BMA–NVP at different surfactant concentrations with the batch addition of an $FeSO_4$/NVP solution. R_p was evaluated according to the previous article,[18] and the results are given in Figure 3. At different Tween 80 concentra-

TABLE II
Comparison of Different Microemulsion Polymerizations of BMA and NVP

Latex	Tween 80 solution (wt %)	SC (%)	Con (%)	Initiator	Particle size	
					R_h (nm)	PDI
Y-525	2.0	12.2	91	BPO–Fe^{2+}	58	0.113
Y-527	3.0	13.3	92	BPO–Fe^{2+}	40	0.102
Y-513	4.0	14.3	92	BPO–Fe^{2+}	27	0.070
Y-511	5.0	15.7	95	BPO–Fe^{2+}	25	0.062
Y-301	6.0	16.4	93	BPO–Fe^{2+}	20	0.065
Y-526	2.0	11.9	89	KPS–Fe^{2+}	48	0.133
Y-528	3.0	12.8	88	KPS–Fe^{2+}	27	0.171
Y-514	4.0	13.7	87	KPS–Fe^{2+}	22	0.179
Y-512	5.0	14.7	87	KPS–Fe^{2+}	19	0.108
Y-221	6.0	16.1	90	KPS–Fe^{2+}	18	0.106

The polymerizations of BMA (5.0 g) and NVP (0.5 g) were carried out in the presence of Tween 80 (3.0 g) and *n*-butanol (0.40 g). The total weight of the latex was 50 g (ref. 18).

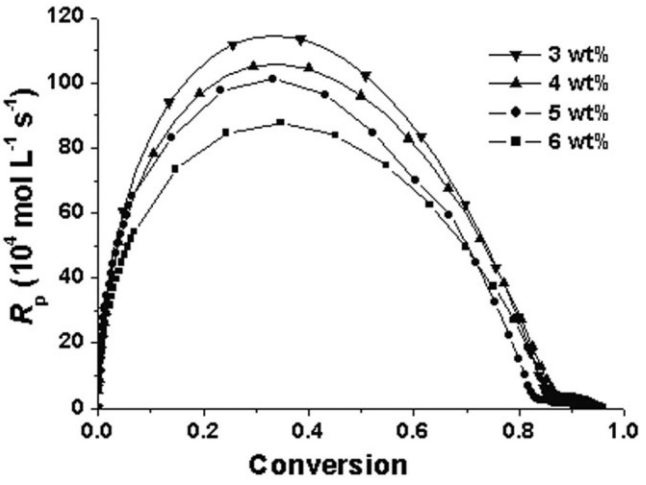

Figure 3 R_p versus the conversion at different surfactant concentrations with the batch addition of an $FeSO_4$/NVP solution: (■) 6, (●) 5, (▲) 4, and (▼) 3 wt %.

TABLE III
Effect of the Surfactant Concentration on the Microemulsion Polymerization of BMA and NVP

Latex	BMA (g)	SC (%)	Con (%)	Initiator	Particle size R_h (nm)	Particle size PDI
Y-535	4.0	14.5	93	BPO–Fe^{2+}	18	0.055
Y-301	5.0	16.4	93	BPO–Fe^{2+}	20	0.064
Y-533	6.5	16.9	77	BPO–Fe^{2+}	48	0.186
Y-529	7.5	17.4	70	BPO–Fe^{2+}	51	0.171
Y-531	10.0	22.7	79	BPO–Fe^{2+}	58	0.164
Y-536	4.0	14.1	88	KPS–Fe^{2+}	17	0.109
Y-221	5.0	16.1	90	KPS–Fe^{2+}	18	0.104
Y-534	6.5	16.5	74	KPS–Fe^{2+}	43	0.157
Y-530	7.5	16.8	67	KPS–Fe^{2+}	48	0.172
Y-532	10.0	22.4	77	KPS–Fe^{2+}	54	0.183

The polymerizations of BMA (5.0 g) and NVP (0.5 g) with different concentrations of Tween 80 were carried out with BPO or KPS (30 mg), $FeSO_4 \cdot 7H_2O$ (40 g), and *n*-butanol (0.40 g) at 40°C. The total weight of the reaction mixture was 50.0 g. The $FeSO_4$/NVP solution was added in a batch.

tions, all the maximum polymerization rates ($R_{p,max}$'s) appeared at about 36% monomer conversion. However, the overall R_p value decreased with the surfactant concentration. On the basis of $R_{p,max}$, the dependence of R_p on the surfactant concentration was estimated to be $R_p \propto [\text{Tween 80}]^{-0.3}$. The reduction of R_p with the surfactant concentration might have resulted from the thickening of the water/oil interface layer and the interruption of the diffusion of the monomer and radical, as suggested by other researchers.[20,21]

Influence of the BMA amount on the interfacially initiated microemulsion polymerization of BMA and NVP

Increasing the solid content in microemulsion polymerization is another research target. We carried out microemulsion polymerizations with different BMA amounts with the batch addition of an $FeSO_4$/NVP solution. When the BMA amount was larger than 5.0 g, the mixtures were translucent, and only two of them (Latex 529 and Latex 531) turned milky after the polymerization. As indicated in Table III, the monomer conversion decreased sharply when the BMA amount exceeded 5.0 g. R_h increased with an increase in the polymerized monomers generally, but there was an abrupt increase between BMA amounts of 5 and 6.5 g. Meanwhile, the particle size distribution became broader in this range. Comparing the results of both polymerizations, we deduced that interfacially initiated microemulsion polymerization led to larger latex particles with narrower size distributions.

The morphology of the latex particles was observed under TEM. The photographs of Latex 531 and 532 are shown in Figure 4, and a core–shell structure can be observed clearly. The coexistence of small and large particles suggested that a large amount of added BMA might induce longer nucleation duration. Unfortunately, it was definitely difficult to observe the core–shell morphology for the smaller latex particles with a low amount of BMA added. We supposed that the small latex made it easy for NVP to diffuse through the particles, and this led to the disappearance of the interface between the two phases for the copolymerization of BMA with NVP. Figure 5 presents the XPS spectrum of Latex 531 particles after extraction with water and reveals the existence of the element N at the electron binding energy of 423 eV, indicating that PNVP was incorporated onto the surface of the latex particles. These results, including FTIR spectra, confirmed the formation of a core–shell structure in the interfacially initiated microemulsion polymerization.

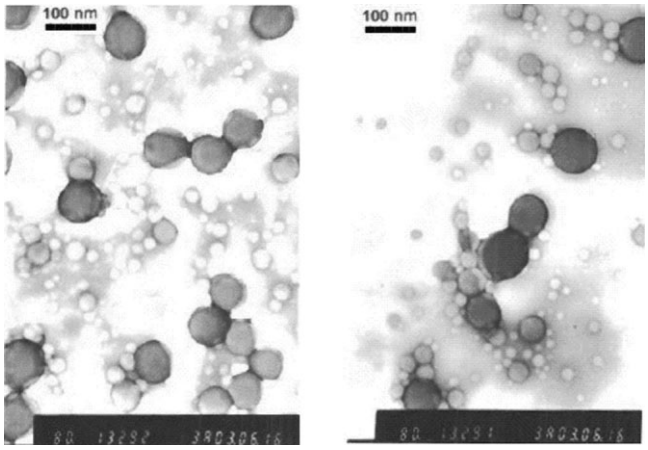

Figure 4 TEM photographs of (a) Latex 529 and (b) Latex 531 particles.

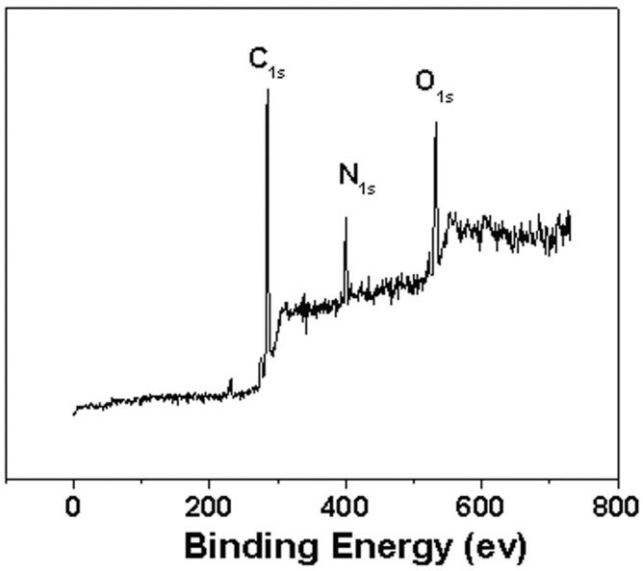

Figure 5 XPS spectrum of Latex 531 particles after extraction with water.

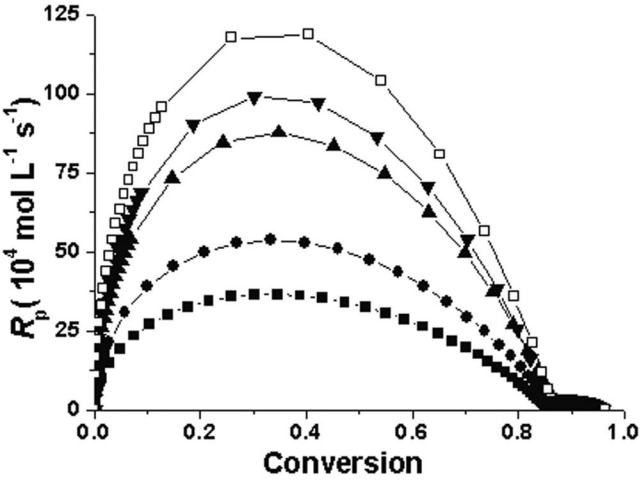

Figure 7 R_p versus the conversion at different temperatures with the batch addition of an $FeSO_4$/NVP solution: (■) 30, (●) 35, (▲) 40, (▼) 45, and (□) 50°C.

Influence of the temperature on the interfacially initiated microemulsion polymerization of BMA/NVP

Raising the polymerization temperature might reduce latex stability and increase R_p and the particle size. Microemulsion polymerizations of BMA (5.0 g) and NVP (0.5 g) were carried out at different temperatures with the batch addition of an $FeSO_4$/NVP solution. The change in the conversion versus the time and that of R_p versus the conversion are shown in Figures 6 and 7, respectively. $R_{p,max}$ in all cases appeared at 36% conversion, and its values increased with the temperature. According to the Arrhenius equation, the apparent activation energy was estimated to be 49.8 kJ/mol on the basis of $R_{p,max}$.

The influence of the polymerization temperature on the particle size and monomer conversion is summarized in Table IV. According to the data in Table IV, the particle size and monomer conversion hardly changed below 40°C. At 40°C, the particle size and monomer conversion increased slightly. Meanwhile, interfacially initiated microemulsion polymerization with BPO–Fe^{2+} resulted in larger latex particles with a narrower size distribution in comparison with noninterfacially initiated microemulsion polymerization with KPS–Fe^{2+}.

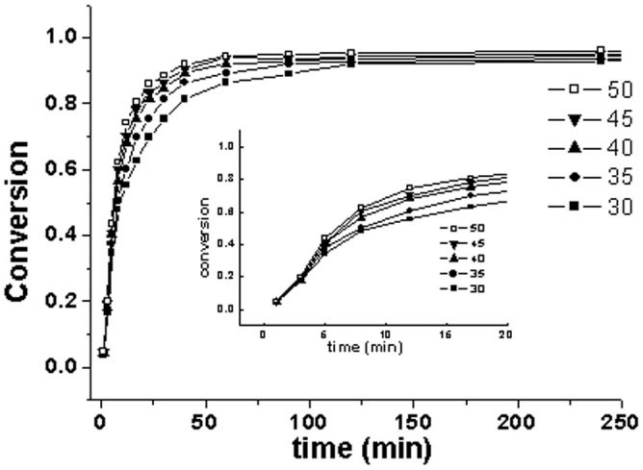

Figure 6 Conversion versus the time at different temperatures with the batch addition of an $FeSO_4$/NVP solution: (■) 30, (●) 35, (▲) 40, (▼) 45, and (□) 50°C.

CONCLUSIONS

With BPO and $FeSO_4$ as the redox initiation couple, the interfacially initiated microemulsion copolymer-

TABLE IV
Effects of the BMA Concentration on the Microemulsion Polymerization of BMA and NVP

Latex	Temperature (°C)	SC (%)	Con (%)	Initiator	Particle size R_h (nm)	Particle size PDI
Y-509	25	15.1	81	BPO–Fe^{2+}	17	0.067
Y-507	30	15.7	87	BPO–Fe^{2+}	18	0.029
Y-505	35	16.1	90	BPO–Fe^{2+}	18	0.069
Y-301	40	16.4	93	BPO–Fe^{2+}	20	0.065
Y-510	25	14.8	79	KPS–Fe^{2+}	14	0.079
Y-508	30	15.2	82	KPS–Fe^{2+}	15	0.102
Y-506	35	15.9	89	KPS–Fe^{2+}	15	0.098
Y-221	40	16.1	90	KPS–Fe^{2+}	18	0.106

The polymerizations of NVP (0.5 g) and different amounts of BMA were carried out with BPO or KPS (30 mg), $FeSO_4 \cdot 7H_2O$ (40 g), Tween 80 (3.00 g), and *n*-butanol (0.40 g) at 40°C. The total weight of the reaction mixture was 50.0 g. The $FeSO_4$/NVP solution was added in a batch.

izations of BMA and NVP were carried out and resulted in core–shell latex particles in one stage. FTIR, XPS, and TEM results demonstrated that the interfacially initiated microemulsion copolymerization facilitated the copolymerization of the oil-soluble BMA monomer with the water-soluble NVP monomer and the formation of the core–shell morphology of the latex particles. The core–shell structure of the PBMA–PNVP latex particles was built in one-stage polymerization. The particle size measurement with DLS showed that the interfacially initiated microemulsion copolymerization produced larger latex particle with a narrower size distribution than the noninterfacially initiated microemulsion copolymerization. With an increase in the surfactant concentration or a decrease in the BMA concentration, PBMA–PNVP latex particles decreased with a slight broadening of the size distribution. Increasing the temperature hardly affected the particle size and its distribution. R_p increased with the temperature but decreased with the surfactant concentration.

The authors thank Qing Wu for the dynamic light scattering measurements.

References

1. Eriksson, S.; Nylen, U.; Rojas, S.; Boutonnet, M. Appl Catal A 2004, 265, 207.
2. Date, A. A.; Patravale, V. B. Curr Opin Colloid Interface Sci 2004, 9, 222.
3. Lopez-Quintela, M. A.; Tojo, C.; Blanco, M. C.; Rio, L. G.; Leis, J. R. Curr Opin Colloid Interface Sci 2004, 9, 264.
4. Hansen, S. H. Electrophoresis 2003, 24, 3900.
5. Capek, I. Adv Colloid Interface Sci 2001, 91, 295.
6. Capek, I. Adv Colloid Interface Sci 2001, 92, 195.
7. Chow, P. Y.; Gan, L. M. Adv Polym Sci 2005, 175, 257.
8. Lopez-Quintela, M. A. Curr Opin Colloid Interface Sci 2003, 8, 137.
9. Capek, I.; Juranicova, V.; Barton, J. Eur Polym J 1999, 35, 691.
10. Badran, A. S.; Nasr, H. E.; All, A. E. M.; El Enany, G. M.; El-Hakim, A. A. J Appl Polym Sci 2000, 77, 1240.
11. Xu, X. J.; Siow, K. S.; Wong, M. K.; Gan, L. M. Langmuir 2001, 17, 4519.
12. Puig, J. E.; Coronagalvan, S.; Maldonado, A.; Schulz, P. C.; Rodriguez, B. E.; Kaler, E. W. J Colloid Interface Sci 1990, 137, 308–310.
13. Pokhriyal, N. K.; Sanghvi, P. G.; Shak, D. O.; Devi, S. Langmuir 2000, 16, 5664.
14. Pokhriyal, N. K.; Devi, S. Eur Polym J 2002, 36, 333.
15. Yun, Y.; Li, H. Q.; Ruckenstein, E. J Colloid Interface Sci 2001, 238, 414.
16. Wang, C. C.; Yu, N. S.; Chen, C. Y.; Kuo, J. F. Polymer 1996, 37, 2509.
17. Yun, Y.; Li, H. Q.; Ruckenstein, E. J Colloid Interface Sci 2001, 238, 414.
18. He, W. D.; Ye, F. M.; Wang, Y. M.; Li, L. F. J Appl Polym Sci 2004, 92, 2334.
19. Wu, C.; Gao, J. In New Developments in Polymer Research; Hu, H. J.; He, T. B., Eds.; Science: Beijing, 1997.
20. Gomez-Cisneros, M.; Trevino, M. E.; Peralta, R. D.; Rabelero, M.; Mendizabal, E.; Puig, J. E.; Cesteros, C.; Lopez, R. G. Polymer 2005, 46, 2900.
21. Capek, I.; Potisk, P. J Polym Sci Part A: Polym Chem 1995, 33, 1675.